Journal of Zhejiang University-SCIENCE C (Computers & Electronics)
ISSN 1869-1951 (Print); ISSN 1869-196X (Online)
www.zju.edu.cn/jzus; www.springerlink.com
E-mail: jzus@zju.edu.cn

Curvature-aware simplification for point-sampled geometry*

Zhi-xun SU†, Zhi-yang LI†‡, Yuan-di ZHAO, Jun-jie CAO

(*School of Mathematical Sciences, Dalian University of Technology, Dalian 116024, China*)

†E-mail: zxsu@hotmail.com; lizy0205@gmail.com

Received Mar. 19, 2010; Revision accepted July 16, 2010; Crosschecked Jan. 31, 2011

Abstract: We propose a novel curvature-aware simplification technique for point-sampled geometry based on the locally optimal projection (LOP) operator. Our algorithm includes two new developments. First, a weight term related to surface variation at each point is introduced to the classic LOP operator. It produces output points with a spatially adaptive distribution. Second, for speeding up the convergence of our method, an initialization process is proposed based on geometry-aware stochastic sampling. Owing to the initialization, the relaxation process achieves a faster convergence rate than those initialized by uniform sampling. Our simplification method possesses a number of distinguishing features. In particular, it provides resilience to noise and outliers, and an intuitively controllable distribution of simplification. Finally, we show the results of our approach with publicly available point cloud data, and compare the results with those obtained using previous methods. Our method outperforms these methods on raw scanned data.

Key words: Point-sampled geometry, Particle simulation, Locally optimal projection, Simplification
doi:10.1631/jzus.C1000068 **Document code:** A **CLC number:** TP391.4

1 Introduction

Point set surface has become a popular surface representation with the development of scanning devices, and 3D modeling and rendering techniques (Alexa *et al.*, 2001; Kobbelt and Botsch, 2004; Guennebaud and Gross, 2007). However, due to physical limitations, the initial output of acquisition devices is generally point clouds with a huge size and varying density. It is important to have tools that adequately adjust the density and optimize the distribution of points (Lipman *et al.*, 2007) in order to facilitate subsequent meaningful processing and visualization.

The works related to simplification for point-sampled geometry are generally categorized as follows: iterative removal methods, clustering methods, and particle-based methods. Most of the first two kinds of methods are fast and easy to implement. However, the distribution of the simplified model is closely linked to the distribution of the original input model (Pauly *et al.*, 2002). Thus, when the original model is poorly distributed (generally caused by some physical measurement process, such as scanning by hand or misalignment of multiple scans), the final simplified model will be poorly distributed. Particle-based methods differ from other methods in that they offer a mechanism for controlling point samples and distributing them according to the needs of the application (Meyer *et al.*, 2005). In particle-based re-sampling of point sampled geometry, the two most often used approaches are sampling on implicit functions (de Figueiredo *et al.*, 1992) and sampling by the moving least square (MLS) projection operator (Pauly *et al.*, 2002).

‡ Corresponding author

* Project (Nos. 60673006 and U0935004) supported by the National Natural Science Foundation of China and an INBRE grant from NIH, USA (No. 5P20RR01647206)

The first approach uses implicit functions to define the underlying surface of the original points, and exploits the well established technique of sampling on implicit functions (Witkin and Heckbert, 1994). However, most of these sampling systems have many parameters that interact with some complexity, making it difficult for users to tune the system to meet specific requirements (Meyer *et al.*, 2005). The second approach, working directly on the point cloud, uses the MLS projection operator to keep the particles on the underlying surface. The operator, however, has the disadvantage of lending too much influence to outliers and cannot deal with the complex geometry well (Lipman *et al.*, 2007). To solve this problem, a parameterization-free locally optimal projection (LOP) operator was proposed by Lipman *et al.* (2007). The output of LOP, a nearly regular distribution point set, is a good approximation of the original surface with proofs. However, a point cloud with spatially adaptive distribution, which is essential for efficient, accurate representations of complex surfaces, cannot be generated using the LOP algorithm.

In this paper, we propose an improved LOP (ALOP) method of curvature adaptive simplification for point-sampled geometry, which means the simplified points should be dense in the high curvature regions, and sparse in the relative planar regions. Due to the effectiveness of classical LOP on raw scanned data (Lipman *et al.*, 2007), our ALOP method is highly robust to noise and outliers and can handle the data with nonuniform distributions and holes. The simplification system also yields an intuitive parameter to control the distribution of the output. One of the well-known difficulties in particle simulation is how to speed up the convergence of the relaxation process. We present a method to place the initial particles in the near-optimal positions, inspired by the geometry-aware stochastic sampling technique (Boubekeur and Alexa, 2009). The relaxation process with this initialization method achieves a faster convergence rate than those initialized by uniform sampling: only about 10 relaxation steps are necessary to obtain an output point with high quality distribution. To evaluate the quality of output points, we have designed a new method for roughly measuring the regularity of points with a spatially adaptive distribution, based on the variance of distances to the adaptive nearest neighbors at the points.

2 Related work

2.1 Surface simplification and re-sampling

A great deal of effort has been undertaken in the last few years, resulting in a variety of point-sampled surfaces simplification algorithms. There are still at least two challenges for a simplification algorithm.

The first is selecting the representative points for simplification. Earlier simplification methods for point-sampled surfaces choose a true subset of the original point cloud as the simplified points. These methods generally assign some kinds of surface error metric value to every point, such as the information content measure (Linsen, 2001), medial axis-related local feature size (Dey *et al.*, 2001), contribution to shape (Alexa *et al.*, 2001), quadric error metrics (Pauly *et al.*, 2002), or confidence map (Pauly *et al.*, 2004). The point with the least value, or the largest value for some methods, is iteratively removed. This kind of algorithm may lead to aliasing artifacts, uneven sampling distributions, or complicated computation (Pauly *et al.*, 2002). An alternative is the clustering method, which splits the point cloud into a number of subsets, and chooses local centroids of the subsets as the representative points. Based on the approaches for building clusters, these methods can be categorized as follows: grid-based method (Alexa *et al.*, 2004), uniform incremental clustering method (Pauly *et al.*, 2002), adaptive hierarchical clustering method (Pauly *et al.*, 2002), principal component analysis (PCA) based method (Kalaiah and Varshney, 2003), adaptive mean-shift clustering method (Miao *et al.*, 2009a), Gauss sphere sampling clustering method (Miao *et al.*, 2009b), etc. The clustering approaches are memory and execution efficient. However, most may cause high approximation errors.

Second, if one does not choose the true subset or local centroids of the original point set during simplification, the other challenge will appear: ensuring the result points near or on the underlying surface. In other words, what is the definition of the underlying surface for the original point set? The generally used definitions are the implicit functions. The radial basis function (RBF) surface (Witkin and Heckbert, 1994; Hart *et al.*, 2005) and the moving least square (MLS) surface are the state-of-the-art methods (Pauly *et al.*, 2002).

2.2 Particle simulation and implicit surface

Implicit surface sampling using particle simulation is a well established technique. It was first introduced by de Figueiredo *et al.* (1992), who used attraction and repulsion forces to create point distributions for polygonization. Following this, a large body of work was developed (Witkin and Heckbert, 1994; Hart *et al.*, 2005; Meyer *et al.*, 2005).

For brevity, we focus on dedicated point cloud simplification algorithms with a particle simulation system. Pauly *et al.* (2002) have proposed using particle systems to simplify point-sampled surfaces. In their method, the MLS surface is defined to adhere to the underlying geometry. To prevent particles from drifting away, particles must be projected onto the surface or the local plane every time the positions are altered. They also proposed an adaptive simulation system by scaling their repulsion radius with the inverse of the local curvature. Meyer *et al.* (2005) used a distance field function of the point cloud as the implicit surface to be sampled, and introduced an interesting new class of energy functions for distributing either uniform or non-uniform particles on the implicit surfaces. Proenca *et al.* (2007) presented methods for fast sampling of point-based multi-level partition of unity (MPU) implicit surfaces using the inner structure of the surface. Their methods work well for different levels of surface complexity and also support shape edits. To better deal with outliers and delicate surface structures, Lipman *et al.* (2007) developed a highly effective, parameterization free projection operator, LOP, which leads to a new underlying geometry definition.

3 The proposed method

Given a surface defined by a point cloud P and a target sampling rate $N < |P|$, the aim of simplification is to find a point cloud Q with $|Q| = N$, such that the distance between the two surfaces Q and P is minimal. In order to generate Q with spatially adaptive distribution, we improve the classic LOP operator by introducing curvature-aware weight terms. As a geometric initialization is necessary for faster convergence of the LOP relaxation, we propose an initialization method considering both curvature and density of every point inspired by a stochastic sampling technique (Boubekeur and Alexa, 2009).

Lipman *et al.* (2007) proposed a framework to solve a problem similar to simplification. The aim is to find a point cloud Q. Q is faithfully adhered to the underlying shape defined by P, and fairly distributed. This framework induces the definition of the desired points Q as the fixed point solution of the equation

$$Q = G(Q), \tag{1}$$

where

$$G(x) = \arg\min_{X=\{x_i\}_{i\in I}} \{E_1(X,P,C) + E_2(X,C)\},$$
$$E_1(X,P,C) = \sum_{i\in I}\sum_{j\in J} \|x_i - p_j\|\theta(\|c_i - p_j\|),$$
$$E_2(X,C) = \sum_{i'\in I}\sum_{i\in I\setminus i'} \eta(\|x_{i'} - c_i\|)\theta(\|c_{i'} - c_i\|).$$

Here $\|\cdot\|$ is the 1-norm, $\theta(r) = \exp(-r^2/(h/4)^2)$ is a rapidly decreasing smooth weight function with a finite support radius defining the size of the influence neighborhood, and $\eta(r) = 1/(3r^3)$ is another decreasing function penalizing x_i that gets too close to other points in X. Thus, the attracting term E_1, related to the multivariate median, is used to project particles on the surface. The repulsing term E_2 is designed to keep the distribution of the points Q fair.

We describe our curvature-aware simplification system in this framework. As mentioned above, the LOP algorithm cannot generate a point set with a spatially adaptive distribution, which is necessary to maintain geometric features during the simplification. To achieve this, new terms that reflect the curvature distribution of the underlying surface should be introduced to Eq. (1). The classical LOP operator localizes the global L_1 median to produce many local L_1 medians by using the finite support weight function $\theta(\cdot)$. To deal with highly non-uniformly distributed models, Huang *et al.* (2009) combined density weights with $\theta(\cdot)$ to improve the regularity of the output. Inspired by these works, we propose to incorporate curvature weights into the terms of the classic LOP. The curvature-aware simplification problem is finally simplified as finding the fixed point solution of the following Eq. (2):

$$Q = G(Q), \tag{2}$$

where

$$G(x) = \arg\min_{X=\{x_i\}_{i\in I}}\{E_1(X,P,C) + E_2(X,C)\},$$

$$E_1(X,P,C) = \sum_{i\in I}\sum_{j\in J}\|x_i - p_j\|\phi_1(\kappa_j)\theta(\|c_i - p_j\|),$$

$$E_2(X,C) = \sum_{i'\in I}\sum_{i\in I\setminus i'}\eta(\|x_{i'} - c_i\|)\phi_2(\kappa_{i'},\kappa_i)\theta(\|c_{i'} - c_i\|).$$

κ_i is the surface variation at the corresponding point in P or Q, reflecting the curvature distribution to some extent. We use the surface variation, but not the curvature in our simplification system, because surface variation is more suitable for simplification of point-sampled surfaces than curvature estimation based on function fitting (Pauly *et al.*, 2002). $\phi_1(\cdot)$ and $\phi_2(\cdot)$ are the curvature-aware weights to control the curvature dependence of the final distribution. Meanwhile, $\phi_2(\cdot)$ controls the regularity in homogeneous regions. The detailed forms of these terms are described in Section 4.2.

We give the iterative solution to Eq. (2) and then analyze the convergence and approximation order of the solution in Section 4.3. However, the number of relaxation iterations, which is necessary for converging into an optimal distribution, remains unknown. It might be sensitive to the initial value most of the time. To obtain a rapid convergence, the initial particles should be placed in the near-optimal states, which are related to the local geometry. We present a method to obtain a good initialization (Section 4.1) based on the geometry-aware random sampling technique proposed by Boubekeur and Alexa (2009). Fig. 1 shows the overview of our simplification algorithm.

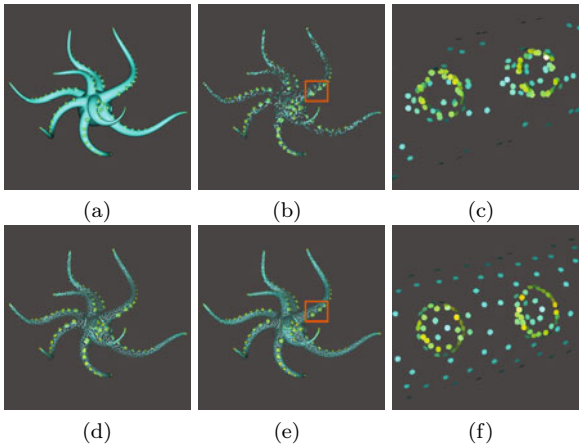

Fig. 1 Overview of the ALOP simplification algorithm: (a) Original Octopus model; (b) Initialization obtained using our geometry-aware stochastic sampling method; (d) Result after 10 ALOP iterations; (e) Result after 30 ALOP iterations; (c, f) Close-up views of (b) and (e), respectively

4 Methodology

4.1 Stochastic point selection

The geometry-aware stochastic sampling technique, proposed by Boubekeur and Alexa (2009), is the initialization method for their mesh simplification process. The sampling technique preserves important geometric features. Point selection prefers areas of high curvatures, but still ensures sufficient sampling in flat parts.

While initializing by this method cannot ensure a uniform distribution in homogeneous regions, which is crucial for fast convergence (Pauly *et al.*, 2002), we incorporate the sampling density of point cloud into stochastic sampling. By sampling more points in regions of lower density, uniformity of the initial sample distribution can be ensured. The initialization algorithm has three steps:

Step 1: Assign two characteristic values κ_i and ρ_i to each point. κ_i is the surface variation at point x_i, and $\rho_i = k/r^2$ is the point density of point x_i, where r is the radius of the enclosing sphere of the k nearest neighbors of x_i.

Step 2: Construct a probability distribution function, defining the probability of the point x_i to appear in the stochastic sampling. The function can also reflect variations on a large scale.

$$F(x_i) = \frac{1}{N}\left(\tilde{k}w_\rho\left(1+\alpha\left(\frac{1/\rho_i}{\text{mean}(1/\rho)}-1\right)\right) + \tilde{k}w_\kappa\left(1+\alpha\left(\frac{\kappa_i}{\text{mean}(\kappa)}-1\right)\right)\right),$$

where N is the number of points in the original point cloud, $\tilde{k}$ is the target simplification number, mean$(\cdot)$ is the arithmetic mean function, and $\alpha \in [0,1]$ is the adaptivity coefficient. We choose $\alpha = 2/3$ for good performance, as Boubekeur and Alexa (2009) suggested. w_ρ and w_κ control the uniformity and curvature dependence of the initial particles distribution, satisfying $w_\rho + w_\kappa = 1$.

Step 3: Iterate over the point cloud P, generate a uniform continuous random variable r supported

on the bounded interval $[0,1]$, for each point $x_i \in P$, and select the point if (and only if) $r < F(x_i)$.

The stochastic point selection method only ensures that the mean number of the initial points is $\tilde{k}$. Thus, it may lead to the number of the points smaller or larger than required. To maintain the number, we randomly insert unselected original points into the initialized points group or remove the points from it.

The initial sampling density could also be changed through adjusting the weights w_ρ and w_κ. Moreover, with a good initialization, the ALOP iteration converges fast. Consider Figs. 2 and 3, for example.

4.2 Curvature-aware weight terms

We discuss the detailed forms and the roles of $\phi_1(\cdot)$ and $\phi_2(\cdot)$. $\phi_1(\cdot)$ should have the ability of attracting more particles in the feature regions, and $\phi_2(\cdot)$ should reduce the repulsing force in the feature regions and ensure the regular distribution of particles in the homogeneous regions. As is well known, in the technique of sampling on implicit functions, the local regularity can be achieved by introducing repulsion amplitude α_i for each particle x_i. We use the form of α_i, as proposed by Meyer *et al.* (2005):

$$\phi_2(\kappa_i, \kappa_{i'}) = (\alpha_i + \alpha_{i'})/2, \tag{3}$$

$$\alpha_i = r + \frac{1}{\kappa_i^d + v}, \tag{4}$$

where α_i is soft scaled by the inverse of the local surface variation value κ_i at x_i. The upper bound on α_i is $1/v$, and the lower bound is r. The bounded value of α_i keeps a minimum distribution in flat regions and prevents from attracting too many particles in high curvature regions (Meyer *et al.*, 2005). Similar to Eq. (4), we define $\phi_1(\cdot)$ as follows:

$$\phi_1(\kappa_j) = \alpha_j, \tag{5}$$

$$\alpha_j = r + \frac{1}{\kappa_j^{-d} + v}. \tag{6}$$

Meyer *et al.* (2005) suggested $v = 0.75$, $r = 0.1$, $d = 2$, and the surface variation κ_i range of $[0, 20]$. It worked well and distributed particles with strong curvature dependence. The curvature dependence of the distribution increased as d increased (Fig. 4).

The roles of $\phi_1(\cdot)$ and $\phi_2(\cdot)$ are explained in the following. For the particles in regions of high curvature, $\phi_1(\cdot)$ increases the attracting force and $\phi_2(\cdot)$ reduces the repulsing force. These two weights cause particles to form denser configurations near these surface features areas. In contrast, in homogeneous regions, as the influence of $\phi_2(\cdot)$ is almost the same, the function $\eta(\cdot)$ dominates in the repulsion term of Eq. (2), making the distribution regular as classic LOP does.

We calculate the surface variation at each point of original points P using the method described in Miao *et al.* (2009a), and rescale it to the interval $[0, 20]$. To reduce the computation time, we assume the value κ_i of the simplified point x_i to be equal to the surface variation value at its nearest point of the point cloud P during the simplification process.

4.3 Convergence and approximation order of ALOP

Lipman *et al.* (2007) presented an iterative solution to the classic LOP operator (Eq. (1)):

$$x_{i'}^{k+1} = \sum_{j\in J} \frac{\alpha_j^{i'} p_j}{\sum_{j\in J} \alpha_j^{i'}} + \mu \sum_{i\in I\setminus\{i'\}} \frac{\beta_i^{i'}(x_{i'}^k - x_i^k)}{\sum_{i\in I\setminus\{i'\}} \beta_i^{i'}}, \tag{7}$$

$$\alpha_j^{i'} = \frac{\theta(\|x_{i'}^k - p_j\|)}{\|x_{i'}^k - p_j\|},$$

$$\beta_i^{i'} = \frac{\theta(\|x_{i'}^k - x_i^k\|)}{\|x_{i'}^k - x_i^k\|} \left|\frac{\partial \eta}{\partial r}(x_{i'}^k - x_i^k)\right|.$$

It is shown that there are two important parameters of the LOP operator. One is h, the support size of the weight function θ. The other is the balancing factor μ. The solution to LOP guarantees an $O(h^2)$ approximation order, if $\mu \in [0, 0.5)$. We obtain the following iterative solution to ALOP (Eq. (2)) with the same process as in Lipman *et al.* (2007):

$$x_{i'}^{k+1} = \sum_{j\in J} \frac{\alpha_j^{i'} \phi_1(\kappa_j) p_j}{\sum_{j\in J} \alpha_j^{i'} \phi_1(\kappa_j)} + \mu \sum_{i\in I\setminus\{i'\}} \frac{\beta_i^{i'} \phi_2(\kappa_{i'}, \kappa_i)(x_{i'}^k - x_i^k)}{\sum_{i\in I\setminus\{i'\}} \beta_i^{i'} \phi_2(\kappa_{i'}, \kappa_i)}. \tag{8}$$

Compared to Eq. (7), Eq. (8) has the same expressions of $\alpha_j^{i'}$ and $\beta_i^{i'}$. The difference is the introduction of the two curvature weights. Thus, if we simply substitute $\alpha_j^{i'}\phi_1(\kappa_j)$ and $\beta_i^{i'}\phi_2(\kappa_{i'}, \kappa_i)$ by $\tilde{\alpha_j^{i'}}$ and $\tilde{\beta_i^{i'}}$ respectively, it is easily proved that our

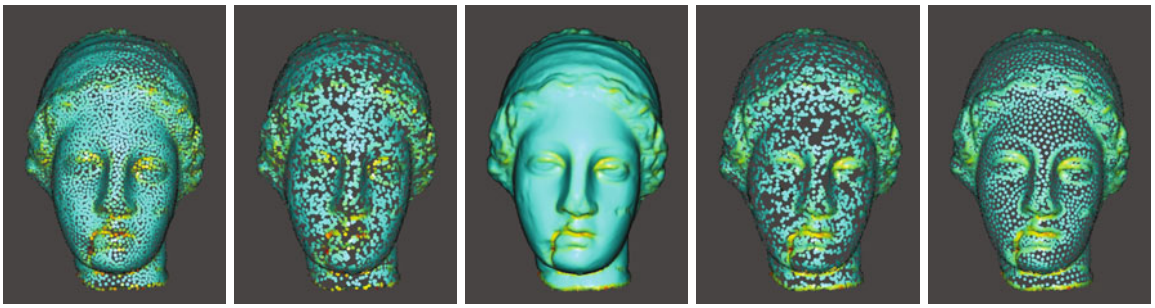

(a) (b) (c) (d) (e)

Fig. 2 Uniform (a, b) and curvature-aware (d, e) simplification on the Igea model. The curvature plot of the model is shown in (c). (a) Result after 10 ALOP iterations with d=0.1; (b) Initialization with w_ρ=1, w_κ=0; (c) Original Igea model; (d) Initialization with w_ρ=1/4, w_κ=3/4; (e) Result after 10 ALOP iterations with d=2

ALOP solution also guarantees an $O(h^2)$ approximation order, based on the conclusion in Lipman *et al.* (2007).

Throughout our experiments, we set $\mu = 0.45$, $h = 4\sqrt{d/M}$, and exploited the forms $\theta(\cdot)$ and $\eta(\cdot)$ as Huang *et al.* (2009) suggested. d is the diagonal length of the bounding box of the input model and M is the number of points in the original model. This choice of parameter values yields both better convergence and a more locally regular point distribution.

5 Results and discussions

In the implementation, we eliminated divisions by zero by adding a very small value to all denominators. All the examples were rendered using the software sview (Adams, 2007), which is shared on the Internet.

All the parameters in our simplification system had the default values. Only two parameters need to be tuned to satisfy different requirements of the simplified model: curvature weight ω_κ in the initialization step, and curvature dependence d in the relaxation step. We set $\omega_\rho = 1/4$, $\omega_\kappa = 3/4$, $d = 2$, and applied 10 iterations in the relaxation step in default cases. The quality of the distribution was advanced with the growth of the number of iterations. α, μ, and h were set as mentioned above, and fixed during the experiments. Our relaxation step had the same number of parameters as the relaxation step of the MLS-based method. However, due to the geometry-aware initialization process, the number of parameters in the whole simplification system was a bit larger than that of the MLS-based method.

In the following subsections, we first describe the roles of the three main parameters in our simplification system via the experiments on different models; next, raw scanned data with noise, outliers, and holes is tested to show the performance of our method; then regularity measure and geometric error analysis are provided to evaluate the regularity and the approximation quality of the simplified model; and finally, we compare our method with the existing methods by testing on raw scanned data and high quality distributed data.

5.1 The two weights in initialization

For all of the results presented in this study, we can initialize our system using the stochastic point selection method as presented above, and maintain the required numbers of particles. Moreover, the distribution of initial sampling points can be adjusted using the weights ω_ρ and ω_κ. These two weights both vary from 0 to 1 and balance the influence of the density and curvature of each point in the initialization process. For example, in Fig. 2, the uniform initialization (Fig. 2b) was sampled with $\omega_\rho = 1$, $\omega_\kappa = 0$, and the curvature-aware initialization (Fig. 2d) was sampled with $\omega_\rho = 1/4$, $\omega_\kappa = 3/4$.

The ALOP iteration converges fast with a good initialization. This was verified experimentally (Fig. 3). The Armadillo model was simplified with initializations obtained by uniform random sampling (Figs. 3a and 3b) and curvature-aware random sampling (Fig. 3c). The latter converged into a near-optimal distribution after about 10 iterations, but the former cannot obtain a comparable distribution

even after 30 iterations. The density of the points in the feature regions in Fig. 3c was higher than those in Figs. 3a and 3b, such as the fingers. And the density of the points in the relative planar regions in Fig. 3c, such as the chest of the model, was more sparse than those in Figs. 3a and 3b.

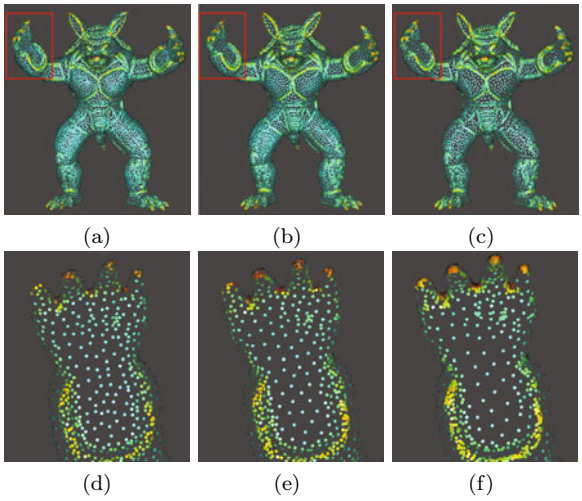

Fig. 3 Fast convergence with a good initialization: the Armadillo model is simplified from 172 974 to 17 226 points. (a) and (b) are the simplification results under uniform initialization (1, 0) with 10 and 30 iterations, respectively; (c) is the result under curvature-aware initialization (1/4, 3/4) after 10 iterations. (d), (e), and (f) are the corresponding close-up views. (c) and (f) have the highest density in the regions of fingers

5.2 Adaptive simplification via curvature dependence parameter *d*

In our proposed framework, the distribution of the output points can be easily controlled by the curvature dependence parameter d, which influences the attracting and repulsing forces intuitively. $d>0$ is a constant value during the simulation stage. $d=2$ generally worked well in our tests to obtain an output with high-quality adaptive distribution. To smooth out the dependence, $d<1$ can be used. In Fig. 4, the Santa model has been simplified from 75 781 points to 7567 points with $d=0.1$, 2, and 10. We can find the differences among them, particularly in the area of high curvature, such as the hand. The ALOP operator distributed more points in high curvature regions and fewer points in relative planar regions, as d increased.

Therefore, by choosing proper weight terms ω_ρ, ω_κ and curvature dependence parameter d, our simplification system can efficiently generate output point sets with distributions from uniform distribution (Fig. 2a) to curvature-aware distribution (Fig. 2e), to satisfy different requirements of the simplified model (see Fig. 2).

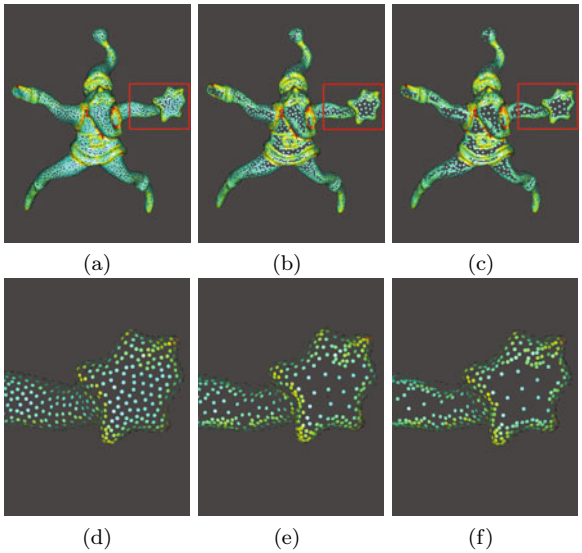

Fig. 4 The effect of varying curvature dependence parameter *d*. (a), (b), and (c) are model simplification by 10 iterations with a varying *d* of 0.1, 2, and 10, respectively; (d), (e), and (f) are the respective close-up views of top row results. The Santa model is simplified from 75 781 to 7567 points

5.3 Coping with noise and outliers

Due to the robust L1 median approximation, our ALOP method is effective in dealing with raw scanned data of complex shapes, and performs well in the simplification of point clouds with noise and outliers.

In Fig. 5, the Face model has been simplified as 5% of the original points. At first, considerable noise and many outliers exist in the original model. The model also has a hole above the eyebrow (Fig. 5a). We filtered the noise and outliers of the original model (Fig. 5d) using the method proposed by Saleem *et al.* (2007), and then performed the ALOP algorithm directly on both the noise model (top row of Fig. 5) and the filtered model (bottom row of Fig. 5). The comparison of results shows that our ALOP algorithm handled noise and outliers well and the hole had little effect on the algorithm. Thus, the ALOP algorithm can be applied directly to raw points.

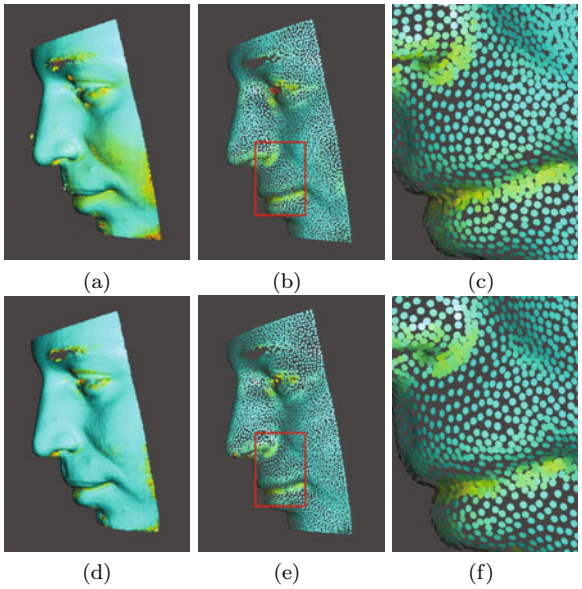

Fig. 5 A face point-cloud with noise and outliers. (a) The Face model consisting of three registered scans; (b) ALOP simplification of (a) via 20 iterations; (c) Close-up views; (d) Filtering the data of (a) by the methods in Saleem *et al.* (2007); (e, f) ALOP simplification result of (d) via 20 iterations and the close-up views, respectively

The noise and outliers in the original point clouds lead to an inaccurate computation of the surface variation for the original points. To alleviate the influence, we computed the surface variation value at each simplified point during the iteration, without assuming the value equal to its nearest point of the original point clouds, as we have suggested before. However, this increased the computation time (as shown later in Table 1). To avoid this, a robust method for the computation of surface variation can be exploited.

5.4 Regularity measure

To evaluate the regularity of the point cloud with curvature-aware distribution, we assume that a high quality point cloud P should have uniform distribution in the homogeneous regions. According to this assumption, a new measure $m(P)$ was carefully designed. The measure is based on the variance of distances to adaptive nearest neighbors at the points:

$$m(P)=\frac{1}{|\Delta|}\sum_{i=1}^{|\Delta|}\sigma(d(p|\kappa(p)\in\Delta_i)), \qquad (9)$$

where Δ is a tagged partition of [0, 20], which is the interval of the scaled surface variation for the point cloud. In the experiment, we particularly generated Δ by uniformly partitioning both the interval [0, 2] and the interval [2, 20] into 20 sub-intervals, because the scaled surface variation values of most points were concentrated on [0, 2]. $d(\cdot)$ denotes the distance between a point and its nearest neighbor in the same sub-interval, and $\sigma(\cdot)$ is a variance function.

The value $m(\cdot)$ roughly measures the regularity in the homogeneous regions, and can be used to compare the quality of results generated by different simplification methods (Section 5.6). The lower value of $m(\cdot)$ reflects the higher quality distribution.

In Fig. 6, we computed the regularity measure of the Octopus model and the Santa model during the relaxation. The figure shows that the simplified points became more and more regular as the number of iterations increased, and it is suitable for us to choose 10 iterations to obtain comparable simplified results.

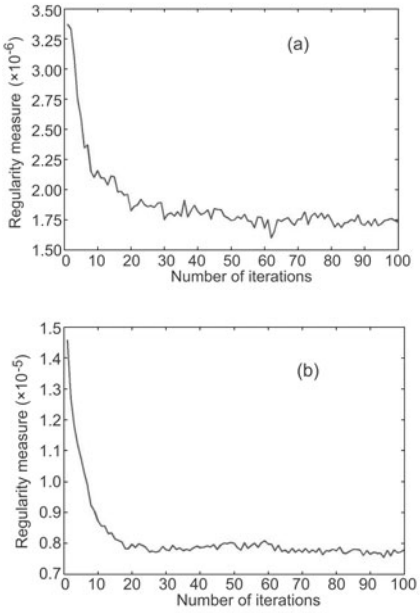

Fig. 6 Plots of the quality value of the Octopus model (a) and Santa model (b) vs. the number of consecutive iterations

5.5 Geometric error analysis

To evaluate the approximation quality of the simplified geometry generated by the ALOP al-

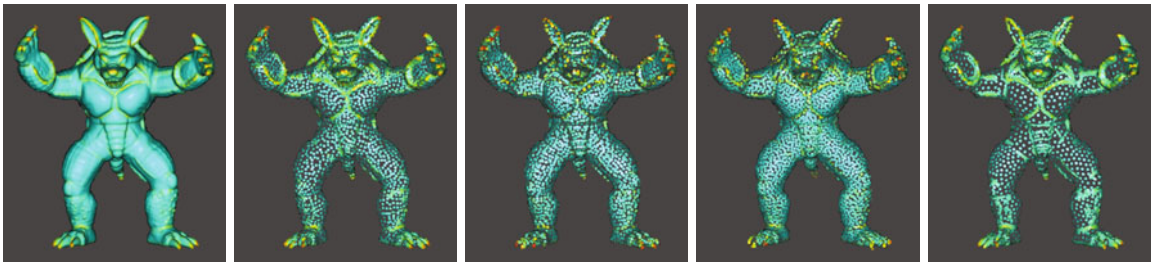

(a) (b) (c) (d) (e)

Fig. 7 Comparison of our simplification method with different methods in the literature on the Armadillo model. (a) The original point cloud model; (b) Hierarchical clustering method (Pauly *et al.*, 2002), (M, T)=(50, 0.01), (Δ_{avg}, m)=(6.86e-4, 3.53e-6); (c) Mean-shift clustering scheme (Miao *et al.*, 2009a), (M, T)=(30, 0.01), (Δ_{avg}, m)=(6.76e-4, 5.87e-6); (d) MLS-based particle simulation method (Pauly *et al.*, 2002), (k, s)=(1, 0.01), (Δ_{avg}, m)=(4.32e-4, 2.73e-6); (e) Our ALOP method, (Δ_{avg}, m)=(4.76e-4, 2.75e-6)

Table 1 Time statistics of the proposed simplification scheme for different point-sampled models

Model	Number of points		Timing*	Normalized	h
	Original	Simplification	(s)	average error	
Igea	134 345	13 227	8.17	3.32e-4	8.70e-3
Santa	75 781	7567	4.56	3.01e-4	1.15e-2
Armadillo	172 974	17 226	10.39	3.45e-4	7.82e-3
Octopus	269 390	8060	5.00	2.31e-4	6.58e-3
Face	84 397	4189	11.90	9.84e-4	1.26e-2
Galaad	1 451 502	14 608	14.14	7.99e-4	3.30e-3

* Collected on a PC with a Core2 Quad 2.33 GHz CPU, 2 GB memory, with 10 iterations

gorithm, we used the geometric average error $\Delta_{\text{avg}}(S, S')$ proposed by Pauly *et al.* (2002) to measure the errors between two surfaces S and S'. The corresponding normalized geometric errors can then be obtained by scaling the above error measures according to the bounding box diagonal of the model. Assuming we have a simplified point cloud P and original point cloud P' representing two surfaces S and S' respectively, then

$$\Delta_{\text{avg}}(S, S') = \frac{1}{|P|}\sum_{q\in P} d(q, S'). \tag{10}$$

$d(q, S')$ is the Hausdorff distance, which is calculated using the MLS projection operator. Table 1 shows the simulation time and geometric error statistics for the example models in this study. Our algorithm was implemented in MATLAB; therefore, it was not yet optimized for speed.

5.6 Comparison with other methods

We compared the simplification results to the existing literature, such as the hierarchical clustering method, mean-shift clustering scheme, and MLS-based particle simulation. We tried our best to adjust the two main parameters of the two clustering methods, maximum cluster size M and maximum curvature threshold T, to achieve the given simplification rate and obtain a curvature-aware distribution. The parameters of repulsion radius r, force constant k, and scale factor s in the MLS-based method were also carefully tuned to increase the repulsive influence, meanwhile preventing the point from drifting away. Our algorithm compared favorably with these methods. It was especially more efficient than these methods when dealing with a raw scanned point set, owing to its parameterization-free and distribution optimized properties.

For input points with high quality distribution (Fig. 7a), the Armadillo model has been simplified to 5% of original points. The ALOP performed well in both the feature regions (see the curvature lines) and the relative planar (see the chest) regions. The points were denser in the high curvature regions while more sparse and regular in the planar regions. The hierarchical clustering method had the highest geometric average error, and our method provided a lower geo-

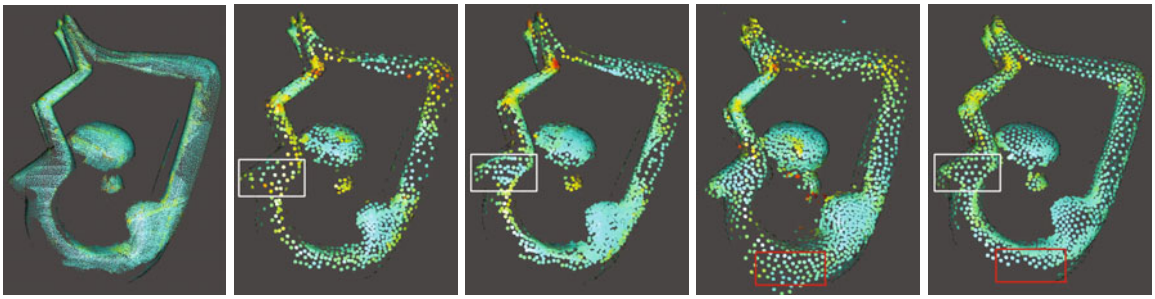

(a) (b) (c) (d) (e)

Fig. 8 Comparison of our simplification method with different methods in the literature on the Indolady model. (a) The original Indolady model; (b) Hierarchical clustering method, (M, T)=(65, 0.025), (Δ_{avg}, m)=(1.0e-3, 4.1e-5); (c) Mean-shift clustering scheme, (M, T)=(50, 0.025), (Δ_{avg}, m)=(2.1e-3, 2.3e-5); (d) MLS-based particle simulation method, (k, s)=(1, 0.01), (Δ_{avg}, m)=(8.8e-3, 3.7e-5); (e) Our ALOP method, (Δ_{avg}, m)=(6.0e-4, 1.1e-5). Our method produces a better distribution for an input raw point set with varying density and boundary

metric error and regularity measure value than these clustering methods.

For the Indolady model with non-uniform distribution and boundary in Fig. 8a, our method redistributed the points in a curvature-aware manner, and provided the lowest geometric error and regularity measure value compared to the listed methods. The density of output points that are simplified by clustering methods was linked to the original points. Take the regions labeled by a box in Figs. 8b and 8c, for example. The MLS-based method cannot deal with this kind of model well, because the geometric information, such as normal, is not well defined on the boundary. As a result, it created points drifting away from the underlying surface (regions labeled by a box in Fig. 8d). In contrast, our method handled the two problems perfectly (Fig. 8e).

6 Conclusions

In this paper, we have described a novel method of curvature-aware simplification for point-sampled geometry using the ALOP operator. Our method handles noise, outliers, non-uniformities, and holes well, all of these being common cases in raw scanned data. The combination of the feature-based initialization and ALOP simulation adaptively reflects the intrinsic property of the underlying 3D model, and provides a faster convergence rate. Our method also yields a simple parameter, which can be used to control the distribution of output points easily and intuitively.

If the input models are high-quality distributed, the ALOP method produces a higher geometric error than the MLS-based methods, due to the approximation limitation of L_1 median. Future research should focus on increasing the approximation order of ALOP and finding a criterion to identify particles that do not need to move.

Acknowledgements

We are grateful to Yong-wei MIAO and Jie-qing FENG for providing the experimental data, and to Bart ADAMS for providing the software sview.

References

Adams, B., 2007. Surfel Viewer. Available from www.cs.kuleuven.be/~barta/sview/sview.html [Accessed on Oct. 18, 2009].

Alexa, M., Behr, J., Cohen-Or, D., Fleishman, S., Levin, D., Silva, C.T., 2001. Point Set Surfaces. Proc. Conf. on Visualization, p.21-28. [doi:10.1109/VISUAL.2001.964489]

Alexa, M., Rusinkiewicz, S., Nehab, D., Shilane, P., 2004. Stratified Point Sampling of 3D Models. Proc. Eurographics Symp. on Point-Based Graphics, p.49-56.

Boubekeur, T., Alexa, M., 2009. Mesh simplification by stochastic sampling and topological clustering. *Comput. Graph.*, **33**(3):241-249. [doi:10.1016/j.cag.2009.03.025]

de Figueiredo, L.H., Gomes, J.D.M., Terzopoulos, D., Velho, L., 1992. Physically-Based Methods for Polygonization of Implicit Surfaces. Proc. Conf. on Graphics Interface, p.250-257.

Dey, T.K., Giesen, J., Hudson, J., 2001. Decimating Samples for Mesh Simplification. Proc. 13th Canadian Conf. on Computational Geometry, p.85-88.

Guennebaud, G., Gross, M., 2007. Algebraic point set surfaces. *ACM Trans. Graph.*, **26**(3):23. [doi:10.1145/1276377.1276406]

Hart, J.C., Bachta, E., Jarosz, W., Fleury, T., 2005. Using Particles to Sample and Control More Complex Implicit Surfaces. ACM SIGGRAPH Courses, p.269-276. [doi:10.1145/1198555.1198657]

Huang, H., Li, D., Zhang, H., Ascher, U., Cohen-Or, D., 2009. Consolidation of Unorganized Point Clouds for Surface Reconstruction. SIGGRAPH, p.1-7. [doi:10.1145/1661412.1618522]

Kalaiah, A., Varshney, A., 2003. Statistical Point Geometry. Proc. Eurographics Symp. on Geometry Processing, p.107-115.

Kobbelt, L., Botsch, M., 2004. A survey of point-based techniques in computer graphics. *Comput. Graph.*, **28**(6):801-814. [doi:10.1016/j.cag.2004.08.009]

Linsen, L., 2001. Point Cloud Representation. Technical Report, Faculty of Computer Science, University of Karlsruhe, Karlsruhe.

Lipman, Y., Cohen-Or, D., Levin, D., Tal-Ezer, H., 2007. Parameterization-free projection for geometry reconstruction. *ACM Trans. Graph.*, **26**(3):22. [doi:10.1145/1276377.1276405]

Meyer, M.D., Georgel, P., Whitaker, R.T., 2005. Robust Particle Systems for Curvature Dependent Sampling of Implicit Surfaces. Proc. Int. Conf. on Shape Modeling and Applications, p.124-133. [doi:10.1109/SMI.2005.41]

Miao, Y., Pajarola, R., Feng, J., 2009a. Curvature-aware adaptive re-sampling for point-sampled geometry. *Comput.-Aided Des.*, **41**(6):395-403. [doi:10.1016/j.cad.2009.01.006]

Miao, Y., Diaz-Gutierrez, P., Pajarola, R., Gopi, M., Feng, J., 2009b. Shape Isophotic Error Metric Controllable Resampling for Point-Sampled Surfaces. IEEE Int. Conf. on Shape Modeling and Applications, p.28-35. [doi:10.1109/SMI.2009.5170160]

Pauly, M., Gross, M., Kobbelt, L.P., 2002. Efficient Simplification of Point-Sampled Surfaces. Proc. Conf. on Visualization, p.163-170. [doi:10.1109/VISUAL.2002.1183771]

Pauly, M., Mitra, N.J., Guibas, L.J., 2004. Uncertainty and Variability in Point Cloud Surface Data. Proc. Eurographics Symp. on Point-Based Graphics, p.77-84.

Proenca, J., Jorge, J., Sousa, M.C., 2007. Sampling Point-Set Implicits. Proc. Eurographics Symp. on Point-Based Graphics, p.11-8.

Saleem, W., Schall, O., Patane, G., Belyaev, A., Seidel, H.P., 2007. On stochastic methods for surface reconstruction. *Vis. Comput.*, **23**(6):381-395. [doi:10.1007/s00371-006-0094-3]

Witkin, A.P., Heckbert, P.S., 1994. Using Particles to Sample and Control Implicit Surfaces. Proc. 21st Annual Conf. on Computer Graphics and Interactive Techniques, p.269-277. [doi:10.1145/192161.192227]